



Transition warming and cooling remanences in magnetite

David J. Dunlop¹

Received 15 June 2007; revised 31 July 2007; accepted 30 August 2007; published 22 November 2007.

[1] Insight into the size and morphology of assemblages of magnetite particles can be gained by comparing temperature variations of remanence or susceptibility after zero-field cooling (ZFC) and after field cooling (FC) through the Verwey transition around $T_V = 120$ K. At 10 K a sample is demagnetized following ZFC, but in the FC initial state before warming the sample has a transition cooling remanence (TrCRM) acquired in crossing T_V . The matching transition warming remanence (TrWRM) acquired as a result of heating a demagnetized sample from low temperature across T_V is often called inverse thermoremanent magnetization (ITRM). In TrCRM experiments, initially demagnetized samples were cooled in a 2 mT field from 300 K to 10 K. Magnetization M was measured at 1 K to 5 K intervals, the highest-resolution data being taken between 140 K and 90 K. The field was zeroed at 10 K, and the TrCRM was monitored during zero-field warming back to 300 K. The properties of TrCRMs are generally similar to those of TrWRMs produced by heating a ZFC sample in a 2 mT field from 10 K. In 10 of 12 samples (grain sizes from 0.6 to 135 μm), M of monoclinic magnetite produced by field cooling through T_V exactly equals M of cubic magnetite produced by field warming through T_V , even though the ultimate TrCRM and TrWRM values when $H \rightarrow 0$ are entirely different. Mirror-image symmetry was observed between in-field warming curves tracking the acquisition of TrWRM and zero-field warming curves of TrCRM between 10 and 300 K. The symmetry, with increases in the field-on M curves mirroring decreases in the field-off M_T curves, was almost perfect from 10 to 110 K. Approximate symmetry was also observed between in-field cooling curves tracking TrCRM production and zero-field cooling curves of TrWRM between 300 K and T_V . Detailed study of the properties and mechanism(s) of transition remanences will help clarify why the ZFC/FC method is diagnostic in some instances and not in others.

Citation: Dunlop, D. J. (2007), Transition warming and cooling remanences in magnetite, *J. Geophys. Res.*, 112, B11103, doi:10.1029/2007JB005233.

1. Introduction

[2] Inverse thermoremanent magnetization (ITRM), discovered by Nagata *et al.* [1963], is produced by heating in a magnetic field through a magnetic phase transition, in magnetite the Verwey transition near $T_V = 120$ K. The properties of ITRM were studied further by Ozima *et al.* [1963], Ozima and Ozima [1965] and Creer and Like [1967]. The latter authors preferred the term transition remanent magnetization, which will be used in this paper. Transition remanence is not limited to warming through a transition. The results described in this paper show that transition cooling remanent magnetization (TrCRM) is a viable reciprocal process to transition warming remanent magnetization (TrWRM) or ITRM in magnetite.

[3] Nagata *et al.* [1963] found that not all TrWRM is produced at T_V . Their sample containing synthetic magnetite

grains several hundred μm in size acquired its largest partial ITRMs near the isotropic point $T_K \approx 130$ K, where the first magnetocrystalline anisotropy constant K_1 of magnetite vanishes. For the samples studied by Dunlop [2006] and used in the present study, the spectrum of blocking temperatures T_B was continuous from 20 to 300 K, with peaks at T_V and T_K . Significant partial ITRM was produced above T_K and below T_V . Any T change that causes an increase in magnetocrystalline anisotropy energy will pin some fraction of the domain walls, locking them in displaced positions when the field is removed [Xu and Merrill, 1992].

[4] The TrWRM fraction produced near T_K in Nagata *et al.*'s [1963] sample was moderately resistant to alternating field (AF) demagnetization, whereas other fractions were much less stable. Understandably the strongest wall pinning will occur close to transitions, where small changes in T result in large changes in K_1 . At T_K , the easy axes change from $\langle 111 \rangle$ to $\langle 100 \rangle$ and K_1 momentarily passes through zero. At T_V , magnetite's structure changes from cubic to monoclinic, with a large increase in anisotropy.

[5] The present work monitors transition remanences produced in both cooling and warming as a continuous function of temperature. The variations with magnetic field

¹Geophysics, Department of Physics, University of Toronto, Toronto, Ontario, Canada.

applied (acquisition curves) are compared with the field-off variations (remanence decay curves). AF stabilities of both TrWRM and the room-temperature memory of TrCRM are also studied as a function of grain size, with and without prior thermal annealing.

[6] One motivation for this research was to better understand the FC (field cooling)/ZFC (zero-field cooling) method of detecting magnetite, particularly chains of biogenic magnetosomes in magnetotactic bacteria [Moskowitz *et al.*, 1993]. The technique compares the temperature variations of induced magnetization/susceptibility (usual in the physics literature) or saturation isothermal remanent magnetization (SIRM) produced at temperatures of 10–20 K following ZFC and FC from 300 K. SIRM and susceptibility warming curves from either state show a clear expression of the Verwey transition. However, the change in FC SIRM across T_V is more than double that of ZFC SIRM for intact magnetosome chains. The difference is small for inorganic crystals and virtually nil for disrupted chains of biogenic crystals.

[7] The mechanism in broad terms is selection of the $\langle 100 \rangle$ axis nearest the applied field as the magnetically easy c-axis in the monoclinic phase below T_V in FC, whereas the c-axis is randomly directed in ZFC [Carter-Stiglitz *et al.*, 2002, 2004]. The effects of elongation of individual crystals (*vis-à-vis* the strong shape anisotropy of crystal chains), particle size dispersion, and oxidation of crystal surfaces are not entirely clear, however.

[8] The present experiments are relevant to the ZFC/FC method because ZFC is the demagnetized state from which TrWRM or ITRM is produced, while FC is the state following production of TrCRM. The experiments described below differ from the usual FC procedure of using a saturating field to ensure selection of the field-favored $\langle 100 \rangle$ axis at T_V . In addition the experiments use pseudo-single-domain (PSD) and multidomain (MD) magnetites, whose response to T_K and T_V depends on domain nucleation and/or wall pinning/unpinning rather than rotation of single-domain (SD) moments.

2. Samples and Experiments

[9] Natural magnetites were prepared by hand crushing large single crystals from Bancroft, Ontario, Canada. Two coarse fractions, 125–150 μm (mean $\sim 135 \mu\text{m}$) and 100–125 μm (mean $\sim 110 \mu\text{m}$), were prepared by sieving and seven fine fractions with mean sizes of 20, 14, 9, 6, 3, 1 and 0.6 μm were separated from the residue using a Bahco dust analyzer. One set of 9 samples was annealed under vacuum at 650–700°C to relieve internal stress, while a second set was left unannealed. All nine annealed magnetites and three of the unannealed samples (0.6, 6 and 20 μm) were used in the present experiments.

[10] SIRM produced at 20 K (ZFC initial state) and measured every 2 K during zero-field warming in an MPMS-2 SQUID magnetometer was almost totally lost at $T_V = 110\text{--}115 \text{ K}$ [Dunlop and Özdemir, 1997, Figure 12.7]. All samples except the 0.6 μm one had reversible weak-field susceptibility χ - T curves (measured with an AGICO Kappabridge), χ dropping to zero just below the magnetite Curie point of 580°C [see Dunlop *et al.*, 2004, Figure 1]. Strong-field thermomagnetic curves measured with a

vibrating-sample magnetometer (PMC microVSM) gave magnetite Curie points for all samples.

[11] The experimental sequence began with 100 mT AF demagnetization at 300 K. The sample was cooled in zero field to 10 K, magnetization being measured every 5 K with the MPMS-2. From this ZFC initial state, a field of 2 mT was switched on and the sample was warmed to 300 K. Magnetization (induced + remanent) was measured every 5 K during field warming (FW), except between 90 K and 140 K, flanking T_V and T_K , where the measurement interval was 1 K. A relatively low field was necessary to ensure that induced magnetization did not overwhelm the details of TrWRM acquisition during warming. At 300 K, the field was switched off and TrWRM was measured. The decay of TrWRM was then measured at 5 K intervals during ZFC back to 10 K.

[12] TrCRM experiments completed the sequence. After zero-field warming (ZFW) to 300 K, samples were AF cleaned to erase TrWRM and then cooled in a 2 mT field from 300 K to 10 K (FC). Magnetizations were measured every 1 K between 140 K and 90 K and every 5 K elsewhere. At 10 K, the field was switched off and TrCRM was measured. Finally, the decay of TrCRM was monitored at 5 K intervals during ZFW back to 300 K.

[13] Stepwise AF demagnetization used 0.5-cm diameter samples containing $\approx 1 \text{ wt\%}$ dispersions of the 1, 6, 20 and 135 μm annealed magnetites, sealed under vacuum in quartz capsules. Samples were individually treated using a Schonstedt demagnetizer with a slow decay rate at low fields. Remanences were measured with a 2G SQUID magnetometer. TrWRM and TrCRM were produced by lowering samples in a plastic basket suspended on threads into a mini-Dewar containing liquid N_2 at 77 K. The sample temperature was allowed to equilibrate for 15 min. The Dewar fit snugly in the bore of a solenoid which in turn fit inside a 3-layer Schonstedt mu-metal shield. The solenoid and shield had their axes vertical and the samples were taped in vertical positions around the inner perimeter of the basket, ensuring axial remanences. The basket could easily be lifted out of the Dewar, whose lid was then replaced and acted as a base for the basket and samples as they warmed rapidly to 300 K.

[14] To produce TrWRM, samples underwent ZFC to 77 K and the solenoid field (1 mT) was switched on just before the samples were removed from the Dewar and left on throughout the warming (FW). TrCRM was produced in a reciprocal procedure. The solenoid field was switched on at 300 K before the samples were lowered into the Dewar (FC). After temperature equilibration, the field was zeroed and the samples warmed to 300 K (ZFW). Most TrCRM demagnetizes in ZFW through T_V , leaving only a small memory of TrCRM at 300 K.

3. MPMS Results

[15] Results for the main experimental sequence are illustrated for four of the 12 samples run. The results for the 6 μm annealed magnetite (Figure 1) are typical of almost all annealed samples. A very small initial remanence after AF cleaning is revealed by a shift in the baseline in ZFC across T_V ($1 \rightarrow 2$). From the ZFC state (2), a field $H = 2 \text{ mT}$ was applied at 10 K, producing an induced magne-

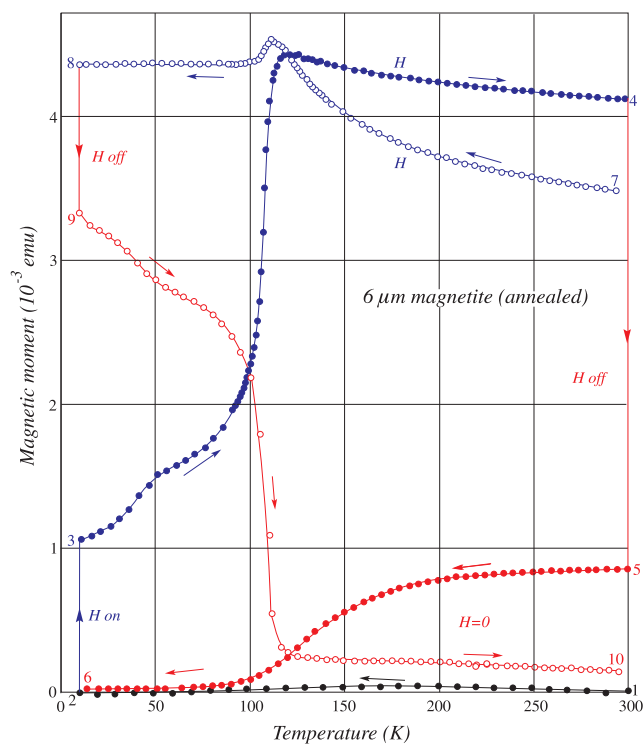


Figure 1. MPMS results for main sequence experiments (6 μm annealed magnetite). TrWRM was produced by FW through T_V (3 \rightarrow 4 \rightarrow 5) and then demagnetized by ZFC (5 \rightarrow 6). TrCRM was produced by FC through T_V (7 \rightarrow 8 \rightarrow 9) and then demagnetized by ZFW (9 \rightarrow 10). Induced magnetizations are equal at 10 K (2 \rightarrow 3, 8 \rightarrow 9) and at 300 K (0 \rightarrow 7, 4 \rightarrow 5). FW and ZFW curves (3 \rightarrow T_V , 9 \rightarrow T_V) and FC and ZFC curves (7 \rightarrow T_V , 5 \rightarrow T_V) are mirror images. Equal M values are produced by FC and FW through T_V .

tization (2 \rightarrow 3). During FW from 10 to 300 K (3 \rightarrow 4) there is a steady increase in magnetization (10–90 K, most marked from 30–50 K), then a large and rapid increase in approaching T_V from below, followed by a gradual decline from a muted Hopkinson peak at 115–120 K. When H is switched off at 300 K, 20% of the magnetization remains as TrWRM (4 \rightarrow 5). Almost all TrWRM is lost at T_V in ZFC (5 \rightarrow 6), completing the cycle.

[16] The TrCRM cycle begins with turning on a 2 mT field at 300 K (7), producing a large induced magnetization. (The preliminary ZFW step from 10 K (6) and AF cleaning at 300 K are not shown.) The magnetization rises much more in FC from 300–110 K than it declined over the same range in FW (3 \rightarrow 4), reaching a sharp Hopkinson peak at 115 K. At and below 100 K, the magnetization in FC is exactly the same as that reached at T_V in FW. When H is switched off at 10 K (8 \rightarrow 9), just over 75% of the magnetization remains as TrCRM. In the final ZFW step (9 \rightarrow 10), most of the TrCRM demagnetizes, from 10–90 K and more precipitously at T_V , leaving only a 3.5% memory at 300 K.

[17] There are a number of striking symmetries in the results of Figure 1. The induced magnetization at 10 K when H is switched on (2 \rightarrow 3) is exactly the same as

magnetization decrease when H is switched off (8 \rightarrow 9). This is somewhat unexpected because the sample is in a ZFC state at 2 but a FC state at 8; there is no a priori reason to suppose domain walls are in the same positions in the two states but it seems to be so. The magnetization increase when H is switched on at 300 K from a ZFW + AF state (from baseline to 7) is also nearly the same as ΔM from a FW state when $H \rightarrow 0$ (4 \rightarrow 5). These observations hint that the direction of temperature change (warming or cooling) is the key factor in the configuration of walls/domains in the state before H is switched on or off. Whether or not H is present during heating or cooling seems to be secondary, i.e., ZFC and FC states seem to be similar and so do ZFW and FW states.

[18] Proceeding from the FC state at 9 and the post-ZFC state at 3, there is almost mirror-image symmetry between the 10–115 K field-on and field-off warming curves. Exactly the same sequence of wall jumps or nucleations must occur in warming with H on or off but in opposite senses (increasing ΔM increments in one case, decreasing ΔM 's in the other). Once again, it is the direction of temperature change that is vital, in this case warming, and not whether or not a field is applied. This result is surprising because, although H is fairly small, internal self-demagnetizing fields are still important. They should produce asymmetry between wall motions or nucleations that reduce M (favored) and those that increase M (opposed).

[19] There is also approximately mirror symmetry between the FC cooling curve from a ZFW + AF state (7 \rightarrow 8) and the ZFC cooling curve from a FW initial state (5 \rightarrow 6). Apart from the Hopkinson peak in the FC curve at T_V , susceptibility variations seem to be minor. The total ΔM from 300 K to T_V is the same in FC and ZFC although the rate of change dM/dT is somewhat different.

[20] The observations that the set of wall motions (or possibly nucleations) in TrWRM acquisition (FW) is reciprocal to that in TrCRM demagnetization (ZFW, 9 \rightarrow 10), and somewhat less exactly, that wall motions in TrCRM acquisition (FC) are reciprocal to those in TrWRM demagnetization (ZFC, 5 \rightarrow 6) do not constitute reciprocity in the sense of Thellier's law of reciprocity of partial TRMs. The set of magnetization increments in FW is not reproduced as magnetization decrements in TrWRM demagnetization during ZFC, probably because the Verwey transition intervenes. Any TrWRM produced in the monoclinic phase leads to a set of domains that must reconfigure in a major way in passing through T_V and T_K , although there is little indication of this in the magnetization curve above T_K until H is zeroed at 300 K, when the bulk of the magnetization is lost (4 \rightarrow 5). It is the reconfigured domains, plus any additional TrWRM acquired above T_K , that demagnetize in ZFC (5 \rightarrow 6).

[21] Just as curve 3 \rightarrow 4 bears no resemblance to curve 5 \rightarrow 6, there is no evidence of reciprocity in the Thellier sense in the FC curve (7 \rightarrow 8) and TrCRM demagnetization in ZFW (9 \rightarrow 10). The Verwey transition resets any domains magnetized between 300 K and T_V , while demagnetization reveals details only for the reconfigured domains in the monoclinic phase between 10 K and T_V .

[22] Results for the 110 μm annealed magnetite (Figure 2) have the same basic pattern. The field-on and field-off induced magnetizations are equal at 10 K (2 \rightarrow 3, 8 \rightarrow 9)

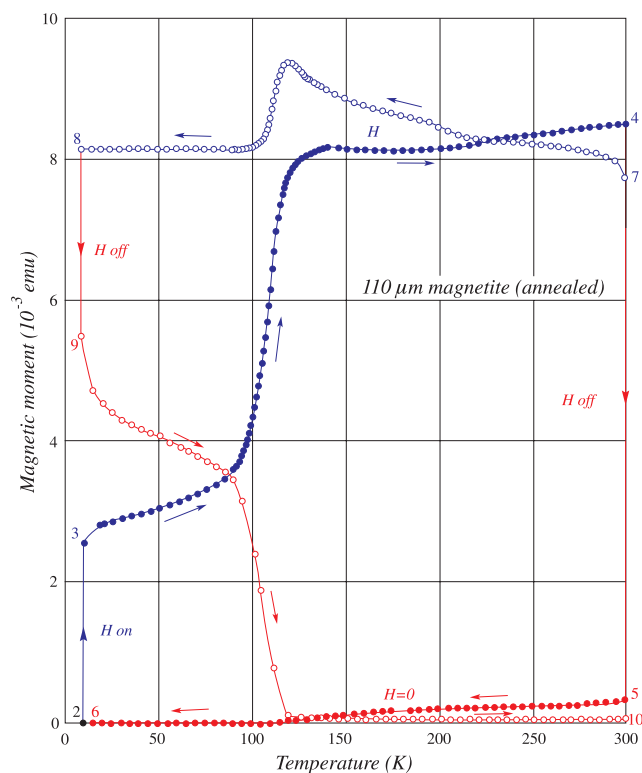


Figure 2. MPMS results for main sequence experiments ($110 \mu\text{m}$ annealed magnetite). The main differences from Figure 1 are a larger Hopkinson peak at and above T_V and consequent lack of mirror symmetry between FC and ZFC curves ($7 \rightarrow T_V$, $5 \rightarrow T_V$).

and also approximately at 300 K ($0 \rightarrow 7$, $4 \rightarrow 5$). The magnetization in FC below 100 K equals that in FW from T_V to 200 K. However, there are some significant differences compared to the $6 \mu\text{m}$ results. The Hopkinson peak in FC is large and not localized at T_V . TrWRM (5) is only 4% of the in-field magnetization at 300 K (4). Decay of TrWRM in ZFC ($5 \rightarrow 6$) from 300 K to T_V does not even approximately mirror the FC curve ($7 \rightarrow 8$) over this range, which seems controlled by χ - T variations culminating in the Hopkinson peak.

[23] Below T_V , TrCRM (9) is about 68% of in-field magnetization at 10 K (8), only slightly reduced compared to the $6 \mu\text{m}$ case. There is approximate but not mirror symmetry between the field-on and field-off warming curves from 10–120 K. From 10–90 K, the decrease ΔM in ZFW of TrCRM (9) is almost double the increase ΔM in FW from a post-ZFC state (3); this may reflect the more important role of the internal self-demagnetizing field in driving walls in these large grains. On the other hand, the rapid increase in M in FW from 90–120 K exactly compensates for this loss: the total ΔM between 10 and 120 K is precisely the same in FW as it is in ZFW.

[24] The $1 \mu\text{m}$ annealed results (Figure 3) have some further novelties. Chief among these is the “scaling up” of the TrCRM cycle (7, 8, 9, 10) compared to the TrWRM cycle (2, 3, 4, 5, 6). M below T_V in the first cycle is 23% greater than M at T_V in the second cycle, giving the pair of

cycles a lopsided aspect. There is no a priori reason why M in high-anisotropy monoclinic magnetite below T_V should equal M in cubic magnetite above T_V . The processes driving walls, the anisotropies, and the easy axes are all different above and below T_V . Nevertheless, the other eight annealed magnetites exhibit this symmetry to within a few percent. The $1 \mu\text{m}$ sample is the sole exception.

[25] Other symmetries are preserved in part for the $1 \mu\text{m}$ sample. From 10–90 K, ΔM in ZFW of TrCRM (9) exactly equals ΔM in FW from a post-ZFC state (3), and moreover the two curves are mirror images in their details. It is above 90 K that the curves lose symmetry, the demagnetization loss much exceeding the magnetization increase in approaching T_V . In cooling from 300 K, the FC curve ($7 \rightarrow T_V$) is approximately a reflection of the ZFC curve of TrWRM ($5 \rightarrow T_V$) but scaled up severalfold.

[26] The results in Figure 4 are typical of the three unannealed samples measured. The other two samples have almost perfect equality of peak M values between TrWRM and TrCRM cycles; only the $20 \mu\text{m}$ sample has unbalanced cycles, the TrWRM cycle in this case having $\approx 10\%$ higher M . The TrWRM cycles of unannealed and annealed samples are generally similar in shape, but the TrCRM cycles of unannealed samples lack the FC Hopkinson peak that is such a prominent feature of $\geq 6 \mu\text{m}$ annealed samples. Mirror image symmetry is not perfect in Figure 4 but the H -on warming process from 25–105 K is basically reciprocal to the H -off warming process over the same interval.

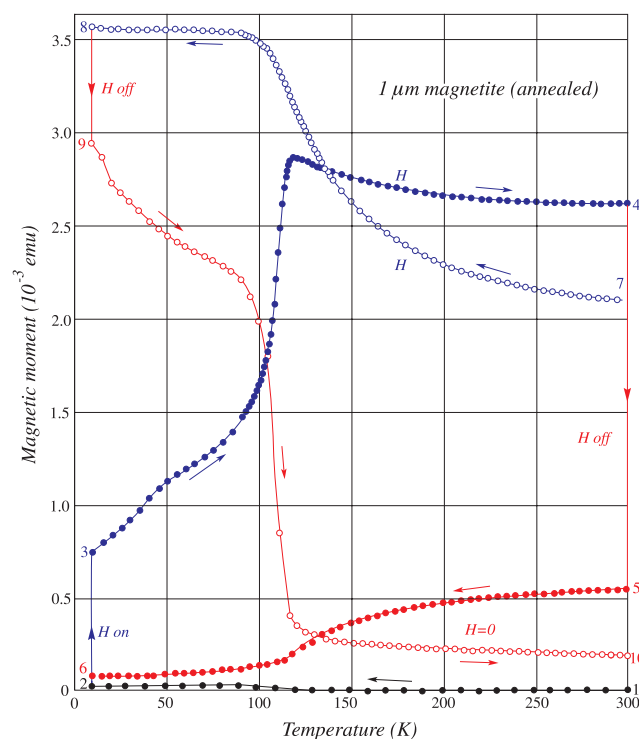


Figure 3. MPMS results for main sequence experiments ($1 \mu\text{m}$ annealed magnetite). New features compared to Figures 1 and 2 are lack of a Hopkinson peak at and above T_V in cooling and asymmetry between the TrWRM and TrCRM cycles: M is much larger after FC through T_V than after FW through T_V .

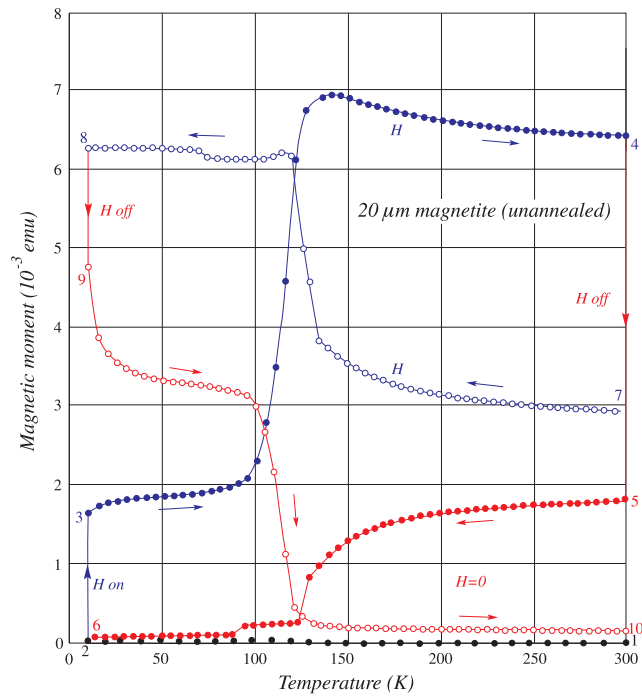


Figure 4. MPMS results for main sequence experiments (20 μm unannealed magnetite). In this sample, mirror symmetries of FW and ZFW curves (3 $\rightarrow T_V$, 9 $\rightarrow T_V$) and of FC and ZFC curves (7 $\rightarrow T_V$, 5 $\rightarrow T_V$) are evident, but M after FC through T_V is somewhat smaller than M after FW through T_V .

Similarly the FC and ZFC cooling processes from 300–130 K have suggestive symmetry, which is interrupted by flux jumps in the SQUID output in both cases. Similar jumps can be seen elsewhere in this figure but they are only

serious when M is changing rapidly because the curves then cannot easily be adjusted to smooth over the jump.

4. Size Dependence and AF Stability of TrCRM and TrWRM

[27] For annealed magnetites, the remanent/total magnetization ratio for TrWRM is only 5–25% after FW from 10 to 300 K (Figure 5). Unannealed grains have ratios about 50% larger than those of annealed grains. TrWRM retains a memory following a single zero-field passage through T_V that ranges from 1/3 in 0.6 and 1 μm annealed grains to nil for $\geq 14 \mu\text{m}$ grains. Memory is ≈ 3 times larger for unannealed grains.

[28] The TrCRM/total magnetization ratio is 65–80% after FC from 300 to 10 K and is only weakly grain size dependent (Figure 6). Annealed and unannealed grains have very similar ratios. The presence or absence of a Hopkinson peak at T_V has no discernible effect on subsequent remanence below T_V . The room-temperature memory of TrCRM after ZFW through T_V has a stronger size dependence. For annealed magnetites, the memory is about 3 times larger for 0.6, 1 and 3 μm grains than for 6, 9, 14 and 20 μm grains (10–15% as opposed to 3–5%) and is negligible for 110 and 135 μm grains. For 1 and 6 μm magnetites, memory is 2–3 times larger for unannealed than for annealed grains. These are similar to documented trends for low-temperature demagnetization (ZFC + ZFW through T_V) of high-temperature remanences like TRM and SIRM [Heider *et al.*, 1992; Halgedahl and Jarrard, 1995].

[29] Stepwise AF demagnetization was carried out for TrWRMs of the 1, 6, 20 and 135 μm annealed magnetites (Figure 7). Median demagnetizing fields (MDFs) range from ≈ 2.5 mT (135 μm) to 4 (20 μm) and 5 mT (1 and 6 μm). The room-temperature memory of TrCRM is con-

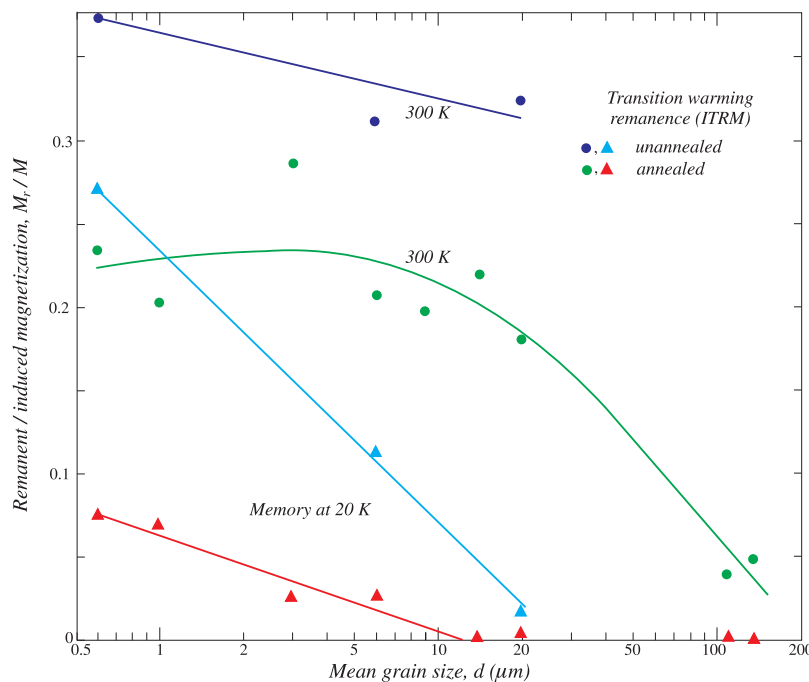


Figure 5. Grain size dependence of remanence ratios of TrWRM (measured at 300 K) and of TrWRM memory (measured at 10 K after ZFC through T_V).

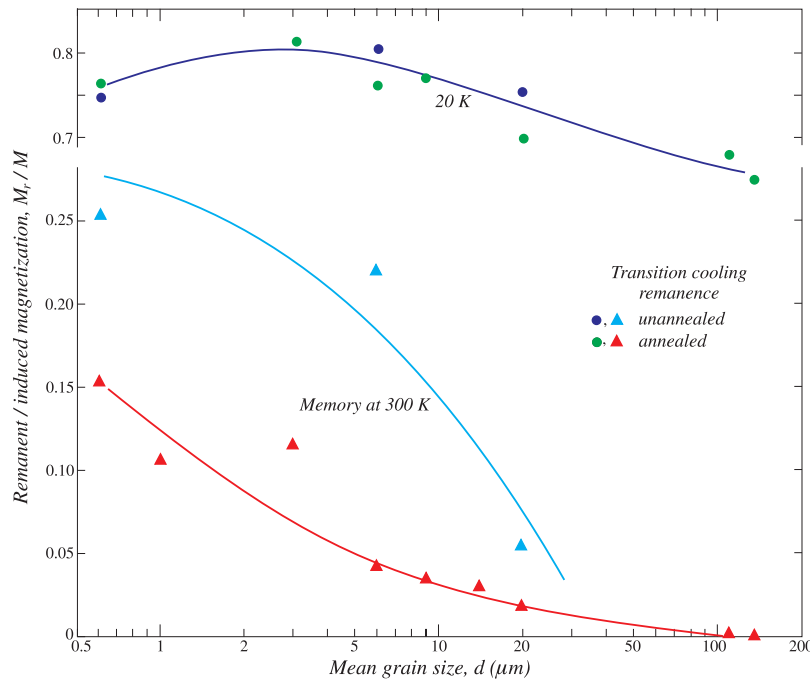


Figure 6. Grain size dependence of remanence ratios of TrCRM (measured at 10 K) and of TrCRM memory (measured at 300 K after ZFW through T_V).

siderably harder (Figure 8). MDFs for the same four samples range from 5 to 15 mT.

5. Discussion

5.1. Behavior Away From Transitions

[30] The blocking mechanism of TrWRM above T_V was interpreted by Nagata *et al.* [1963] to be progressive pinning of domain walls due to increases in magnetocrystal-

line anisotropy K_1 with changing T . Walls narrow as K_1 increases and are more effectively pinned by lattice defects. TrWRM blocks during heating and unblocks during cooling because K_1 increases from 0 at T_K to a peak just below room temperature T_0 [Dunlop and Özdemir, 1997, chap. 3]. Demagnetization by cooling has been studied in some detail in developing stepwise LTD [Dunlop, 2003] and the inverse Thellier method of determining paleointensity [Dunlop and

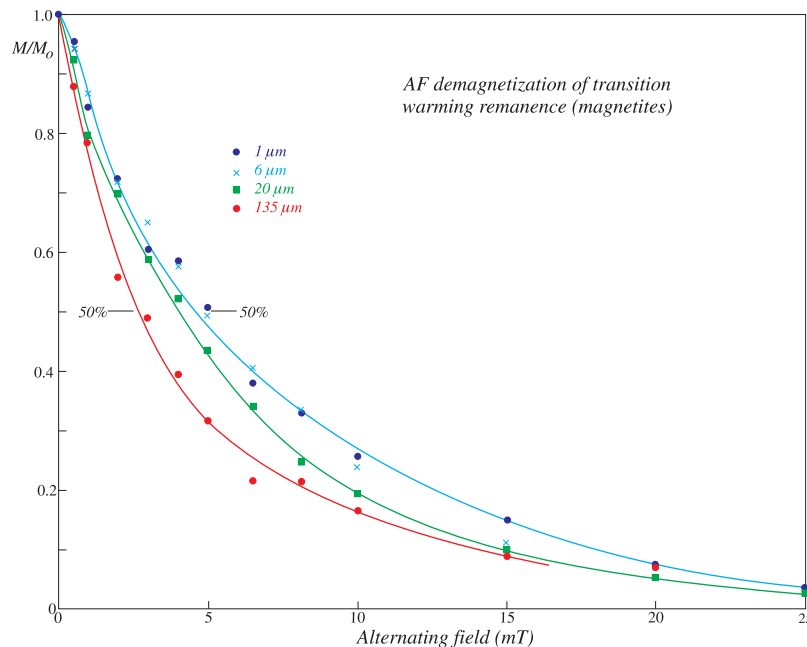


Figure 7. Stepwise AF demagnetization of TrWRM (1, 6, 20, and 135 μm annealed grains).

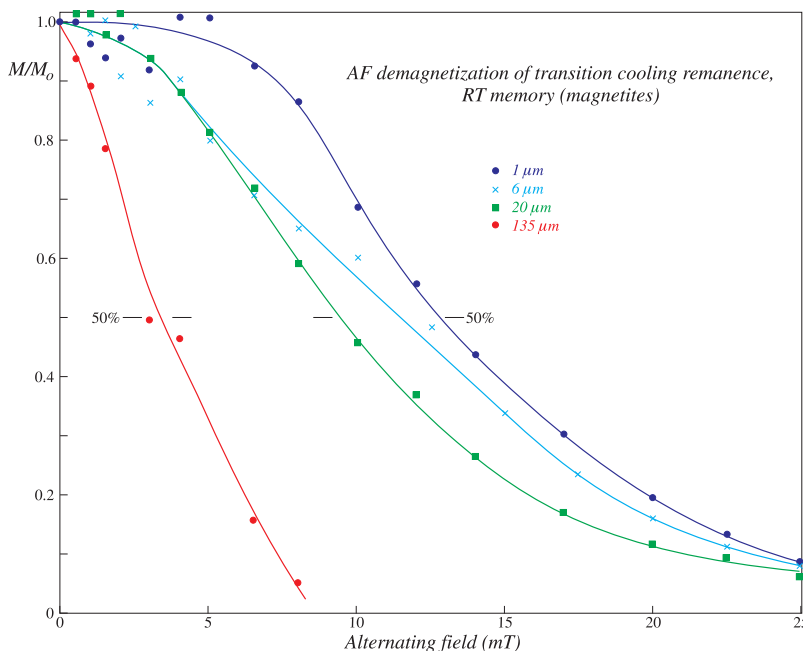


Figure 8. Stepwise AF demagnetization of TrCRM memory after ZFW through T_V .

Yu, 2003]. Acquisition of TrWRM in some of the same samples above T_K was revealed by partial remanences acquired over limited T intervals [Dunlop, 2006] but is not so evident in the present results with continuous FW across T_V . Only in the $110 \mu\text{m}$ (Figure 2) and $135 \mu\text{m}$ (not illustrated) annealed samples does the FW curve rise from T_V to T_0 (4). In the other samples, χ must decrease sufficiently in moving away from the Hopkinson peak at T_V to mask any acquisition of TrWRM. The other possibility is that virtually all TrWRM is produced in domain renucleation and/or reordering at T_V . TrWRM definitely has unblocking temperatures between T_V and T_0 , as expressed in the ZFC curves from T_0 (5) to T_V for all samples.

[31] What of the continuous rise in the FC curve from T_0 (7) to T_V ? The approximate mirror symmetry with the ZFC curve implies reciprocal sets of wall displacements (nucleations are unlikely with small changes in K_1) but irreversible displacements in FC are ruled out because K_1 is decreasing over this range and so is the magnetostriction λ_{111} [Dunlop and Özdemir, 1997, chap. 3], so TrCRM cannot be blocked between T_0 and T_V . If we follow the FC curve below T_V , it is absolutely flat for all samples, implying no change in either reversible or irreversible magnetization. We are led to the conclusion that all TrCRM is truly a transition remanence, acquired at or near T_V and T_K . This is the case whether there is a peak at T_V (Figures 1 and 2) or not (Figures 3 and 4).

[32] Below T_V , Abe *et al.* [1976] found that the anisotropy constants of monoclinic magnetite change slowly from 4 to 60–80 K but more rapidly (and monotonically) from 80–120 K. The dominant constant K_a (which is ≈ 20 times K_1 of cubic magnetite at T_0) decreases with heating but other terms increase or even reverse sign. Magnetostriction constants λ change rapidly from 80–100 K, the general effect being an increased magnitude with increasing T [Tsuya *et*

al., 1977]. Özdemir [2000] and Özdemir *et al.* [2002] reported small ($\leq 10\%$) reversible increases in coercive force H_c of two single crystals between 20 and 120 K. Despite the observations of increasing K , λ and H_c , walls evidently unpin irreversibly in ZFW: for all samples, TrCRM steadily drops between 10 K (9) and T_V , especially above 80 K.

[33] Now we must address the mirror-image FW curve from 10 K (3) to T_V . There is almost perfect reciprocity between ZFW and FW wall jumps over at least part of this range for all samples. The only difference is the direction of the jumps. Since walls are progressively unpinning in both cases, any TrWRM acquired during FW should be lost if H were to be turned off below T_V . In reality, some partial remanence can be acquired and retained below T_V [Dunlop, 2006, Figures 1–4] but the bulk is produced above 100 K.

5.2. Behavior Near T_V and T_K

[34] The increases in M in approaching T_V from below in FW and from above in FC can be spectacular (e.g., Figures 3 and 4) but the configuration of walls must be largely reset in crossing the transition. Halgedahl and Jarrard [1995] measured Barkhausen jumps in M of a natural single crystal using a SQUID magnetometer, during an LTD cycle (ZFC + ZFW) from 260 K to 70 K and back and also in the course of FC in a -1 mT field, both from an SIRM initial state. Most jumps were in the expected direction (decrease in M) but in a “wild zone” from 110–112 K, there were some very large jumps in the opposite direction in both ZFC and FC, so that M actually increased across the transition.

[35] Halgedahl and Jarrard [1995] observed no large changes in M around $T_K = 130$ K, where domains change from $\langle 111 \rangle$ to $\langle 100 \rangle$ easy axes and the walls presumably reconfigure accordingly. Instead, the largest changes were around T_V , where an existing cubic $\langle 100 \rangle$ axis is selected as the monoclinic easy c -axis. In FC, even in fairly small

fields, the body domains and their bounding walls normally parallel the field as closely as possible, so that the rotation of domains and walls would be expected to be minimal across T_V if the field-favored $\langle 100 \rangle$ axis is selected. In ZFC, there is no guiding field at either T_K or T_V . However, the major change should again be at T_K where the domains must rotate a minimum of 71° and not at T_V where the already occupied $\langle 100 \rangle$ axis would logically dictate the choice of monoclinic easy axis. If this reasoning is faulty, and domain orientation (with accompanying magnetostriction, shortening the occupied $\langle 100 \rangle$ axis) is not by itself enough to determine the monoclinic c-axis without an accompanying field, there is no evidence of it in *Halgedahl and Jarrard's* [1995] results. The Barkhausen jumps across T_V look the same in ZFC and FC. Likewise the present results show identical ΔM 's from ZFC and FC states at 10 K and very similar (but mirror reflected) changes of M from 10 to 110 K in either case (Figures 1–4).

[36] Domain observations of the monoclinic phase of magnetite at low temperature were made by *Moloni et al.* [1996] using magnetic force microscopy (MFM). The crystal was cut and polished parallel to a $\{110\}$ plane, which contains one $\langle 100 \rangle$ and two $\langle 111 \rangle$ axes. At 300 K, a cubic pattern of $\langle 111 \rangle$ body and closure domains with 180° , 109° and 71° walls was observed. Below T_V , two styles of domain structure appeared: (1) straight 180° walls bounding domains parallel to the in-plane $\langle 100 \rangle$ axis and (2) wavy walls with reverse spikes due to uniaxial anisotropy with out-of-plane $\langle 100 \rangle$ easy axes. The two styles were seen in adjacent areas of a $20 \mu\text{m} \times 20 \mu\text{m}$ image, showing that different easy axes were selected on this scale in cooling through T_V , although the relationship between sets of domains above and below T_V is unclear. In warming from 77 K, the patterns did not change appreciably until they vanished at 111 K. After recooling to 77 K, the style was similar but walls had moved slightly from their previous pins. Wavy patterns changed more than lamellar domains. The complete disappearance of domain structures implies a more profound reorganization than reorientation of existing domains in crossing T_V . Unfortunately it was not possible in the MFM experiments to observe renucleation of domain structure as the sample warmed above T_V .

[37] Some insight comes from experiments by *Özdemir and Dunlop* [1999]. SIRM was produced at 300 K by a field applied along a $\langle 100 \rangle$ axis of their large single crystal and M was measured along the same axis. 85% of the SIRM demagnetized in ZFC to T_K . There was no further demagnetization between T_K and T_V . In crossing T_V , M increased by an amount exceeding the original SIRM. Results for an unoriented crystal resembled those of *Halgedahl and Jarrard* [1995]: the SIRM demagnetization was not so clearly associated with T_K and the remanence increase across T_V was much smaller. Thus changes occurring between T_K and T_V and in crossing T_V are only clearly revealed if observations are made along $\langle 100 \rangle$, the cubic and monoclinic easy axis appropriate for that temperature range.

[38] The present experiments offer no obvious clues to the microscopic processes that cause M to change across T_V . Section 5.1 concluded that TrCRM is produced entirely, and TrWRM mainly, by domains reorganizing or nucleating in the presence of the 2 mT field at T_V . TrCRM measured at

10 K (point 9 in Figures 1–4) constitutes 65–80% of the total M in annealed and unannealed magnetites of all sizes from $0.6 \mu\text{m}$ (small PSD) to $135 \mu\text{m}$ (large MD). The changes in cooling through T_V must be profound, probably a complete renucleation of domains, in order to generate and block such major remanence. Yet the crossing of the Verwey transition in FC is marked only by a fairly small peak ($\leq 15\%$ of M) in the larger annealed grains (Figures 1 and 2) and no peak or discontinuity at all in the unannealed and finer annealed grains (Figures 3 and 4). In general terms, it is unclear why domain structure should collapse and renucleate at T_V . The monoclinic structure is only slightly deformed with respect to the cubic structure and the easy c-axis below T_V makes an angle of only 0.2° with the cubic $\langle 100 \rangle$ easy axis [*Abe et al.*, 1976].

[39] The FW curves are no more informative about what happens in warming through T_V . Although M reaches a maximum near 120 K (1 and $6 \mu\text{m}$, Figures 1 and 3) or 130 K (20 and $110 \mu\text{m}$, Figures 2 and 4), there is no well-marked peak or sharp change in any sample. The random orientation of crystalline axes in these samples may blur details of changes in M along specific axes. Microscopically, collapse of the monoclinic domain structure and renucleation of cubic domains, along or near $\langle 100 \rangle$ in both phases, must be occurring in all grains. This process is reciprocal to what occurs during cooling in TrCRM production but it is not at all clear why the total magnetization M produced in passing from cubic \rightarrow monoclinic should be exactly the same (in 10 of 12 samples) as that produced in passing from monoclinic \rightarrow cubic. Anisotropies and domain structures are completely different for the two phases, as well as the fraction of M ultimately retained as remanence at 10 K or 300 K when $H \rightarrow 0$.

5.3. Size Dependence and AF Stability

[40] Although the magnetites span a wide range of PSD and MD sizes, TrWRM remanence ratios M_r/M are almost size independent: 0.2–0.25 for the 0.6 – $20 \mu\text{m}$ annealed samples and about 50% higher than this for unannealed samples (Figure 5). Only for 110 and $135 \mu\text{m}$ grains does M_r/M drop to the low values usually considered characteristic of MD grains (≈ 0.05). Although all the magnetites must contain domain walls, except possibly some grains in the $0.6 \mu\text{m}$ sample, there is a definite PSD-MD threshold evident in the efficiency of acquiring TrWRM. On the other hand, the TrWRM memory at 20 K after ZFC through T_V is strongly size dependent and drops to zero for $20 \mu\text{m}$ and larger grains. This is puzzling because it implies that the domain processes that occur in ZFC and in the earlier FW through T_V are not reciprocal (although the previous section concluded that the processes in FC and FW through T_V are reciprocal). The higher anisotropy of the monoclinic phase would logically have a stabilizing effect but the opposite seems to be true. Even more puzzling, the memory at 300 K after a complete LTD cycle (ZFC followed by ZFW) is much less size dependent than the 20 K memory, and the $20 \mu\text{m}$ and larger annealed grains with zero 20 K memory somehow recover $\approx 10\%$ of their original TrWRM intensity in ZFW to 300 K [*Dunlop*, 2006, Figure 6].

[41] TrCRM remanence ratios are also weakly size dependent but much larger than those of TrWRM: 0.65–0.8 for annealed and unannealed grains of all sizes

(Figure 6). Remanence pinning efficiencies in FC and FW through T_V differ by factors ranging from ≈ 2 for $0.6 \mu\text{m}$ unannealed grains to >10 for 110 and $135 \mu\text{m}$ grains. The larger remanence ratios may reflect the much higher anisotropy of the monoclinic phase, which limits the number of walls since wall energy $\sim K^{1/2}$. Large MD grains should have fewer walls and broader domains below T_V than above and the smallest grains might approach SD behavior, with very high remanence ratios. However, measured domain widths of $8.5 \mu\text{m}$ (77 K) and $\approx 10 \mu\text{m}$ (99 K) [Moloni *et al.*, 1996] are not very different from widths in cubic magnetite [Özdemir and Dunlop, 2006, Figure 13]. The high anisotropy may overshadow magnetoelastic effects; this may be the reason why annealed (low stress) and unannealed (higher stress) grains have similar TrCRMs. At 300 K, because of the much lower anisotropy of cubic magnetite, TrCRM memory is both size dependent and much lower for annealed than for unannealed grains (Figure 6). This picture is not entirely convincing, however, because TrWRM memory of the monoclinic phase at 10 K is also size dependent and much lower for annealed than for unannealed grains (Figure 5).

[42] TrWRM is easily AF demagnetized for all grain sizes (Figure 7), in contrast to the pronounced size dependence of AF demagnetization curves of weak-field TRM for the same samples [Dunlop *et al.*, 2004, Figure 2]. All curves in Figure 7 have an exponential MD aspect but the MDFs are even less than for $135 \mu\text{m}$ TRM. The displaced walls responsible for TrWRM must be less strongly pinned after FW through T_V and T_K than they are in FC from the Curie point. The room-temperature memory of TrCRM after FC + ZFW through T_V and T_K is much more resistant to AF cleaning (Figure 8). In fact, the shapes and MDFs of the 1, 6 and $20 \mu\text{m}$ demagnetization curves are comparable to those of the corresponding TRM demagnetization curves.

[43] TrCRM in the monoclinic phase would be expected to have strong pinning of walls at stress centers such as twin boundaries between regions of the crystal having different c-axes but this source of high coercivity disappears on warming through T_V . Although the mechanism is not known, TrCRM produced in monoclinic magnetite is able to target sites of strong pinning in the cubic phase similar to those that pin TRM but quite different from those that pin TrWRM upon FW through T_V .

6. Conclusions

[44] All 9 annealed and 3 unannealed magnetites tested, spanning the range of small PSD to large MD sizes (0.6 to $135 \mu\text{m}$), acquired both TrWRM and TrCRM in passing through the isotropic temperature T_K and the Verwey transition at T_V . TrWRM produced by field warming through these transitions in magnetite has been known since the 1960s [Nagata *et al.*, 1963] but the reciprocal remanence TrCRM resulting from field cooling through the same transitions has not been described previously.

[45] The warming or cooling of the two remanences in zero field makes it clear that TrCRM unblocks (in warming) entirely below and at T_V , while TrWRM unblocks (in cooling) only above T_K and in crossing T_K and T_V . The blocking ranges are not entirely compatible with the unblocking ranges. TrCRM seems to be produced entirely

in field cooling through T_V and not at all in field cooling from T_V to 10 K. TrWRM is blocked mostly at T_V and T_K , with a much smaller fraction of blocking temperatures between T_K and room temperature T_0 .

[46] TrCRM blocking in monoclinic magnetite is very efficient. 65–80% of M produced in crossing T_V remains as remanence when $H \rightarrow 0$ at 10 K. TrWRM of cubic magnetite is much less efficient. For annealed magnetites, only 5–25% of M produced in crossing T_V remains as remanence when $H \rightarrow 0$ at 300 K, large MD grains having the smallest values.

[47] The memories of TrCRM and TrWRM, although carried by different phases of magnetite with very different anisotropies, are quite similar in their magnitudes and size dependences, possibly because each involves one warming and one cooling through T_V and T_K . The TrWRM memory at 20 K and the TrCRM memory at 300 K both range from $\approx 25\%$ (unannealed) or $\approx 10\%$ (annealed) for 0.6 and $1 \mu\text{m}$ grains to 2–5% for $20 \mu\text{m}$ grains and zero for 110 and $135 \mu\text{m}$ grains.

[48] TrWRM has very low resistance to AF cleaning; MDFs are ≤ 5 mT for all grain sizes. TrCRM memory is more resistant, with MDFs around 10–12 mT and somewhat SD-like curve shapes for 1–20 μm grains.

[49] The most interesting results of this study are the symmetries between field-on + field-off warming/cooling (or cooling/warming) cycles of TrWRM and TrCRM. The symmetries include (1) equal values of induced magnetization from different initial states when H is turned on/off at 10 K and 300 K; (2) equal values of total M produced in field cooling and in field warming across T_V for 10 of 12 samples; (3) mirror-image symmetry, ranging from nearly perfect to approximate, between warming curves from 10 K to T_V for zero-field demagnetization of TrCRM (FC initial state) and in-field TrWRM acquisition from a ZFC initial state; and (4) for most samples, good to approximate mirror-image symmetry between cooling curves from 300 K to T_V for zero-field demagnetization of TrWRM (FW initial state) and in-field TrCRM acquisition from a ZFW initial state.

[50] These symmetries imply that during warming, domain walls make the same set of jumps, either toward or away from a demagnetized state, whether or not a field is acting and independent of initial state (ZFC or FC). The same is approximately true for cooling from T_0 to T_V .

[51] However, reciprocity in the sense of the Thellier laws is not exhibited by TrWRM and TrCRM continuously monitored over the 10–300 K range. The acquisition curve of TrWRM (in-field warming) and the zero-field cooling curve of TrWRM are not even approximately symmetric. The acquisition curve of TrCRM (in-field cooling) and the zero-field warming curve of TrCRM are likewise not symmetric. The reason for the failure of reciprocity is that almost all remanence is blocked in crossing transitions and not above or below T_V , whereas unblocking occurs continuously with changing T .

[52] **Acknowledgments.** Helpful comments by Bruce Moskowitz and an anonymous reviewer improved the paper. Measurements were made at the Institute for Rock Magnetism, which is funded by the University of Minnesota, the Earth Sciences Division of NSF, and the Keck Foundation. Thanks to Jim Marvin, Mike Jackson, and Peat Sølheid for help with the

experimental setup and data acquisition. This research was supported by NSERC Canada grant A7709.

References

- Abe, K., Y. Miyamoto, and S. Chikazumi (1976), Magnetocrystalline anisotropy of low temperature phase of magnetite, *J. Phys. Soc. Jpn.*, *41*, 1894–1902.
- Carter-Stiglitz, B., M. Jackson, and B. Moskowitz (2002), Low-temperature remanence in stable single domain magnetite, *Geophys. Res. Lett.*, *29*(7), 1129, doi:10.1029/2001GL014197.
- Carter-Stiglitz, B., B. Moskowitz, and M. Jackson (2004), More on the low-temperature magnetism of stable single domain magnetite: Reversibility and non-stoichiometry, *Geophys. Res. Lett.*, *31*, L06606, doi:10.1029/2003GL019155.
- Creer, K. M., and C. B. Like (1967), A low temperature investigation of the natural remanent magnetization of several igneous rocks, *Geophys. J. R. Astron. Soc.*, *12*, 301–312.
- Dunlop, D. J. (2003), Stepwise and continuous low-temperature demagnetization, *Geophys. Res. Lett.*, *30*(11), 1582, doi:10.1029/2003GL017268.
- Dunlop, D. J. (2006), Inverse thermoremanent magnetization, *J. Geophys. Res.*, *111*, B12S02, doi:10.1029/2006JB004572.
- Dunlop, D. J., and Ö. Özdemir (1997), *Rock Magnetism: Fundamentals and Frontiers*, 573 pp., Cambridge Univ. Press, New York.
- Dunlop, D. J., and Y. Yu (2003), Testing an inverse Thellier method of paleointensity determination, *J. Geophys. Res.*, *108*(B9), 2447, doi:10.1029/2003JB002469.
- Dunlop, D. J., S. Xu, and F. Heider (2004), Alternating field demagnetization, single-domain-like memory, and the Lowrie-Fuller test of multidomain magnetite grains (0.6–356 μm), *J. Geophys. Res.*, *109*, B07102, doi:10.1029/2004JB003006.
- Halgedahl, S. L., and R. D. Jarrard (1995), Low-temperature behavior of single-domain through multidomain magnetite, *Earth Planet. Sci. Lett.*, *130*, 127–139.
- Heider, F., D. J. Dunlop, and H. C. Soffel (1992), Low-temperature and alternating field demagnetization of saturation remanence and thermoremanence in magnetite grains (0.037 μm to 5 mm), *J. Geophys. Res.*, *97*, 9371–9381.
- Moloni, K., B. M. Moskowitz, and E. D. Dahlberg (1996), Domain structure in single crystal magnetite below the Verwey transition as observed with a low-temperature magnetic force microscope, *Geophys. Res. Lett.*, *23*, 2851–2854.
- Moskowitz, B. M., R. B. Frankel, and D. A. Bazylinski (1993), Rock magnetic criteria for the detection of biogenic magnetite, *Earth Planet. Sci. Lett.*, *120*, 283–300.
- Nagata, T., M. Ozima, and M. Yama-ai (1963), Demonstration of the production of a new type of remanent magnetization: Inversed type of thermoremanent magnetization, *Nature*, *197*, 444–445.
- Özdemir, Ö. (2000), Coercive force of single crystals of magnetite at low temperatures, *Geophys. J. Int.*, *141*, 351–356.
- Özdemir, Ö., and D. J. Dunlop (1999), Low-temperature properties of a single crystal of magnetite oriented along principal magnetic axes, *Earth Planet. Sci. Lett.*, *165*, 229–239.
- Özdemir, Ö., and D. J. Dunlop (2006), Magnetic domain observations on magnetite crystals in biotite and hornblende grains, *J. Geophys. Res.*, *111*, B06103, doi:10.1029/2005JB004090.
- Özdemir, Ö., D. J. Dunlop, and B. M. Moskowitz (2002), Changes in remanence, coercivity and domain state at low temperature in magnetite, *Earth Planet. Sci. Lett.*, *194*, 343–358.
- Ozima, M., and M. Ozima (1965), Origin of thermoremanent magnetization, *J. Geophys. Res.*, *70*, 1363–1369.
- Ozima, M., M. Ozima, and T. Nagata (1963), Role of crystalline anisotropy energy on the acquisition of stable remanent magnetization: Inverse type of thermoremanent magnetization, *Pure Appl. Geophys.*, *55*, 77–90.
- Tsuya, N., K. I. Arai, and K. Ohmori (1977), Effect of magnetoelastic coupling on the anisotropy of magnetite below the transition temperature, *Physica B*, *86-88*, 959–960.
- Xu, S., and R. T. Merrill (1992), Stress, grain size and magnetic stability of magnetite, *J. Geophys. Res.*, *97*, 4321–4329.

D. J. Dunlop, Geophysics, Department of Physics, University of Toronto, Toronto, ON, Canada M5S 1A7. (dunlop@physics.utoronto.ca)